

Detection and Velocimetry of Floating Wood for Flood Disaster Risk Management using Electromagnetic Imaging

Christopher Gomez ^{1,2,*}, Norifumi Hotta ³, Shusuke Miyata ⁴, Balazs Bradak ¹, Mikito Kataoka, ¹ Kensuke Ashikaga ¹, and Frans C. Persendt ⁶

¹ Kobe University, Faculty of Oceanology, Sabo Laboratory, Kobe City, Japan; C.G.; christopher-gomez@bear.kobe-u.ac.jp

² Gadjah Mada University, Centre of Natural Hazards and Disaster Risk, Indonesia; C.G.;

³ University of Tokyo, Graduate School of Agricultural and Life Sciences, Department of Forest Science; N.H.; hotta.norifumi@fr.a.u-tokyo.ac.jp

⁴ Kyoto University, Disaster Prevention Research Institute Kyoto, Japan; S.M.; miyata.shusuke.2e@kyoto-u.ac.jp

⁵ University of Namibia, Centre for Innovation in Learning and Teaching, Windhoek, Namibia; F.P.; fpersendt@unam.na

* Correspondence: kaikikazanbear@gmail.com;

Abstract: Wood travelling in river is a major hazard to lives and infrastructures, because tons of wood material can travel nearing the speed of the flood-flow. If post-event mapping, detection and numerical simulation have made important progress, detecting in-flow driftwood in all weather and at all-time still presents several challenges. The present work aims to expand the capacity to detect in-flow wood by adapting the Ground Penetrating Radar electromagnetic method. The laboratory test was carried over a water circulation flume using an 800 MHz nominal frequency antenna sampling at 100 Hz and a video-camera set on top of the flume to measure the average velocity of the wood logs. A set of single wood logs of 20 cm length travelled underneath the antenna. The GPR results have demonstrated that the method had the potential to detect moving wood, and that it could “see” underneath the water to the shallow flume floor. The experiments resulted in the ability to count wood travelling underneath the antenna, and instantaneous velocity were obtained with velocities ranging from 0.307 to 0.352 m/s, which slightly higher than the averaged velocity measured from video-imaging. This difference is explained by in-flow acceleration of the wood after its introduction in the flume.

Keywords: Wood; Driftwood; In-flow Wood Monitoring; Radar; River; Flood

Citation: Christopher Gomez, Norifumi Hotta, Shusuke Miyata, Balazs Bradak, Mikito Kataoka, Kensuke Ashikaga, Frans C. Persendt. Detection and Velocimetry of Floating Wood for Flood Disaster Risk Management using Electromagnetic Imaging *Proceedings* **2022**, *69*, x. <https://doi.org/10.3390/xxxxx>

Academic Editor: Firstname Lastname

Published: date

Publisher’s Note: MDPI stays neutral with regard to jurisdictional claims in published maps and institutional affiliations.



Copyright: © 2022 by the authors. Submitted for possible open access publication under the terms and conditions of the Creative Commons Attribution (CC BY) license (<https://creativecommons.org/licenses/by/4.0/>).

1. Introduction

Wood located in channels and within the riverbed (Figure 1) have been demonstrated to play an essential geomorphic role on natural habitats [1], often putting ecological and economic goals in competition. Indeed, during the historical periods, industrialized countries have been systematically clearing logjams from large waterways, as they can increase flooding and disrupt economic activities relying on waterways [2]. From a scientific and management perspective, wood also provides a proxy of the recruitment process in a river catchment, notably through the depositional patterns in the floodplain (i.e. single large of small pieces, single or racked jams...) [3]. The size and the location of the wood in the stream is in turn exerting a control on the alternation between deposition and transport, with the mountain streams preferentially transporting wood during floods [4,5,6], while larger streams and rivers can also carry wood at mode flow [5]. The characterization and volume estimation of the wood in the floodplain and in the waterways is mostly occurring

in the aftermath of wood travel and transport. It is done for wood trapped in water reservoirs behind dams using data from volume removed by the hydro-electric companies [7]; using historical and time-lapse cameras [7], using geometric calculations from field photographs of the deposits [8], and using digitization from post-flood deposits [9]. Even field research on the flowage of wood is dominated by work on deposited material [10], and the entrainment [11] and movement data are often obtained from laboratory and computer simulations [12,13,14].



Figure 1. Wood in rivers of East Asia: (a) Grounded debris in the Barumun River (Sumatra, Indonesia); (b) Wood trapped in artificially reworked pointbars in the Tamagawa River (Tokyo, Japan); (c) Wood logs deposited in the swale of a pointbar in South-Taiwan (China); (d) wood logs trapped inside a Sediment check-dam (sabo-dam) in the Sumiyoshigawa river, Kobe, Japan; (e) wood in a mountain stream of Gifu Prefecture (Japan); (f) a mountain stream of Aichi Prefecture (Japan); and wood deposited by a pyroclastic-flow and exhumed as a terrace in Numazawa (Japan).

In the field, the in-flow log-displacement have been resolved using RFID and GPS tracking devices implanted in, or chained to the logs [14], allowing the authors to link the driftwood incipient motion to a 40% bankfull discharge notably.

However, wood monitoring using video cameras and photographs have been shown to be challenging in poor visibility conditions (even if positive results have been obtained at night under the right lighting conditions [15]), and most of the work relying on post-event imaging [16]. Another issue, which is still unresolved, is for logjams and logs travelling underneath the water-surface. To bridge this research-gap, it is thus necessary to develop a monitoring method that can retrieve information at night, in the rain, and for material underneath the water. One instrument that is known to work at frequencies travelling in the air, the ground and freshwater is Ground Penetrating Radar, and inverting the GPR variable to solve, the technique can be adapted to moving objects, like RADAR detects planes in the sky.

Ground Penetrating Radar (GPR) is an electromagnetic method based on the propagation of electromagnetic waves in the ground. The antenna emits an electromagnetic signal, which is then propagated through the ground, mostly in relation to the dielectric permittivity of the material. The later varies with a variety of factors (rock type, grain-size, amount of water, the presence of iron oxides, water, etc.), in such a way that the electromagnetic wave in a vacuum travelling at 0.3 m/ns travels at values usually beneath 1/3 of the velocity in a vacuum. The GPR is made of a signal generation and control system linked to an antenna with a nominal electromagnetic frequency ranging from 10 MHz to ~1000 MHz. The imaging of the studied medium is carried out by dragging the GPR antenna over the surface of a target, which then provides a representation of the internal structure of this medium. This image relies on the returned electric part of the electromagnetic signal. The ability of radar to penetrate media beyond travelling the air was randomly discovered by the US Air force when flying over Greenland and crashing into the ice, because the radar did not return the ice level, but the bedrock underneath. From this accident, researchers started to develop GPR to image the ice thickness, characteristics [17] as well as the ice and snow levels and density [18], before turning to soils and river environments: deposits architecture and related processes [19], floodplain structure [20], and faults through the floodplains [21], landslides' displacements [22], etc. GPR work also extended on the coastlines [23], as well as more challenging environment in term of data acquisition and processing, such as debris-flow deposits [24] and still-warm (600 degrees) pyroclastic flow deposits [25]. Outside of the field of geosciences, high-frequency antenna have been also instrumental when hatched to a truck to monitor highways' pavement [26], bridge structures, and tunnels [27], etc. All this research relies on a multitude of radar impulses stacked next to one another, in order to image the internal architecture of an object, but there has also been research with the GPR antenna being kept immobile, in order to investigate the change of the radar signal: e.g. the relation between GPR signal and snow wetness [28].

Nevertheless, there has not been any research on GPR applied to moving water-flows and moving objects in water. Instead of moving the antenna over a known distance, the space-time relation can be determined using the physics of electromagnetic waves. In the present contribution, we aim to prove that GPR technology can be used for the purpose of wood detection and velocimetry in challenging environment, when it has not been possible to acquire direct data from other sensors or from sensors attached to the driftwood [13, 14].

2. Experimental setup and methodology

In the present research, a Ground-Penetrating Radar Mala Reflex-ProX mounted with an antenna of nominal frequency of 800 MHz, was set over a 0.2 m wide water circulation flume at 0.28 m above the water, which is 0.1425 m deep just underneath the antenna

(Figure 2). The geometry of the water underneath during the flow has a cross-sectional area of 0.0285 m² and a wetted perimeter of 0.485 m for a slope of 0.00435 m/m. The wood section used in the present case are 0.2 m long and have a diameter of 0.008 m (Table 1). The average velocity of the driftwood was measured using the time between two points in the flume from video-imagery. The video-camera was located above the flume.

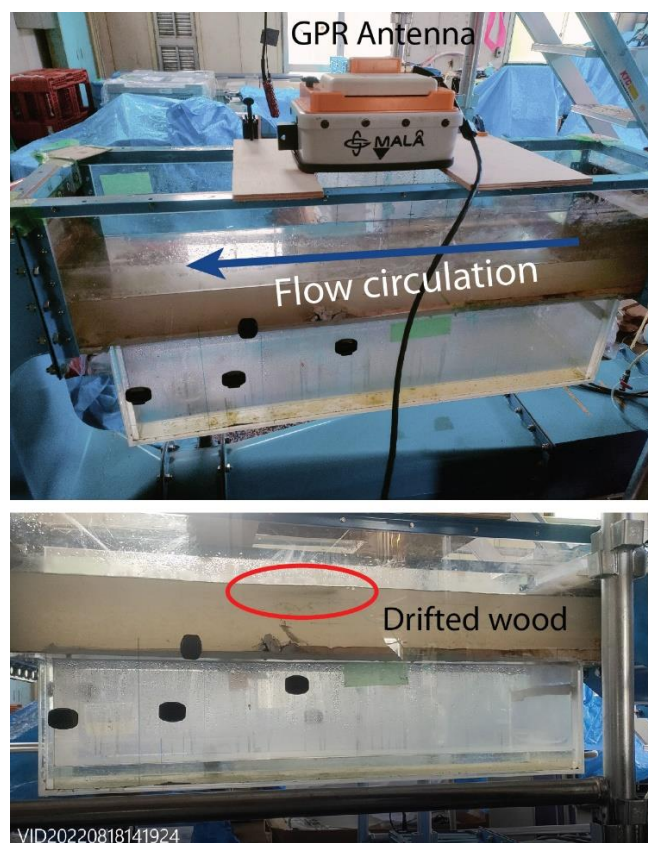


Figure 2. Instrumental setup in the laboratory with the driftwood being released and transported by the water underneath the 800 MHz antenna.

Table 1. Characteristics of the floated wood as well as the Manning water velocity estimates.

<i>Floating wood characteristics</i>					<i>Manning calculation of velocity and discharge</i>					
<i>total length</i>	<i>Wood ϕ</i>	<i>Wood L.</i>	<i>Wood Area</i>	<i>Velocity</i>	<i>Wetted Area</i>	<i>perimeter</i>	<i>Slope</i>	<i>n (artificial laminated Chow,1959)</i>	<i>Velocity</i>	<i>Discharge</i>
[m]	[m]	[m]	[m ²]	[m/s]	[m ²]	[m]	[m/m]	[/]	[m/s]	[m ³ /s]
1.15	0.008	0.2	0.01	0.25	0.0285	0.485	0.00435	0.02	0.50	0.01
1.15	0.008	0.2	0.01	0.2	0.0285	0.485	0.00435	0.02	0.50	0.01
1.15	0.008	0.2	0.01	0.25	0.0285	0.485	0.00435	0.02	0.50	0.01
1.15	0.008	0.2	0.01	0.25	0.0285	0.485	0.00435	0.02	0.50	0.01
1.15	0.008	0.2	0.01	0.25	0.0285	0.485	0.00435	0.02	0.50	0.01
1.15	0.008	0.2	0.01	0.2	0.0285	0.485	0.00435	0.02	0.50	0.01

The radargram was recorded in *rd3, and from one single radargram, the six wood length that floated underneath the radar were confirmed from videos and soundtracks. The portion of the radargram was then exported to (1) remove the antenna to water surface region, so that the time 0 of each trace is at the water surface. (2) the DEWOW filter was applied to limit the effect of the surface penetration and (3) horizontal repeats and noise were suppressed using a signal average removal, for which the average was calculated from every 100 traces (the choice was purely empirical, and based on the quality of different trial and error). Moreover, (4) the signal amplitude was enhanced using the AGC gain. Finally, (5), using the known velocity of electromagnetic waves in fresh water (0.033 m/ns), the time of the returned signal was transformed into the depth of penetration (by also halving the two-way signal).

From the set of processing steps above, one has a set of hyperbolae created by the wood moving towards, and away from the antenna. This is represented on the radargram by the traditional hyperbolae signals. Instead of attempting to calculate the velocity of the signal in the medium by relating the horizontal distance to the time it takes to reach a certain depth, the authors turned the method upside down and used the known velocity in the air/vacuum (not in the water because the travel from the antenna to the wood is controlled by the travel in the air) to calculate the distance travelled for a known time-span in the air. This data was then converted into the velocity of each wood.

3. Results and discussion

For the 6 wood samples, the observed wood velocity over a flume length of 1.1 m varied between 0.2 to 0.25 m/s, although these values are certainly underestimated as the wood was still being accelerated towards an equilibrium velocity. By comparison, the estimation made from the Manning’s equation, which provided a water velocity of 0.49 m/s. (Table 2).

Table 2. Wood velocity calculation from the videos and numbering relating to the GPR hyperbolae

<i>Wood velocity from videos</i>										
<i>Nb</i>	<i>GPR</i>	<i>M Setup</i>	<i>Water depth</i>	<i>Wood velocity</i>	<i>In</i>	<i>Out</i>	<i>Distance</i>	<i>Time</i>	<i>Up-stream depth</i>	<i>Down-stream depth</i>
[/]	[/]	[/]	[m]	[m/s]	[sec]	[sec]	[m]	[sec]	[m]	[m]
1	8	75	0.1425	0.25	14	18	1	4	0.145	0.14
2	8	75	0.1425	0.2	19	24	1	5	0.145	0.14
3	8	75	0.1425	0.25	26	30	1	4	0.145	0.14
4	8	75	0.1425	0.25	31	35	1	4	0.145	0.14
5	8	75	0.1425	0.25	36	40	1	4	0.145	0.14
6	8	75	0.1425	0.2	41	44	0.6	3	0.145	0.14

* Nb is the Number; M Setup is the Motor Setup; In and Out signifies the time when the wood was introduced and left the measurement area; the Distance is the distance travelled by the wood for velocity calculation.

The 800 MHz GPR signal penetrated the water to the flume floor 0.1425 m underneath the water level (Figure 3). The depth was confirmed by plunging a ruler in the flume water. Due to the preparation time, the first wood only passes underneath the antenna after 140 seconds, while the last one passes slightly after 170 seconds (Figure 3). The 6 wood, although only 0.008 m in diameter created a clear signal and as they did not flow

in a straight line, but realigned themselves, it resulted in hyperbolae with several “heads” (further comparison is needed between video and the GPR signal). For each hyperbola the velocity calculation from the rising limb of the hyperbola (as the wood was still being accelerated, it explains why the falling limb is having a slight different angle) provided velocities ranging from 0.307 to 0.380 m/s (Table 3), which is higher than the velocities recorded from the video data (0.2 to 0.25 m/ns of averaged velocity).

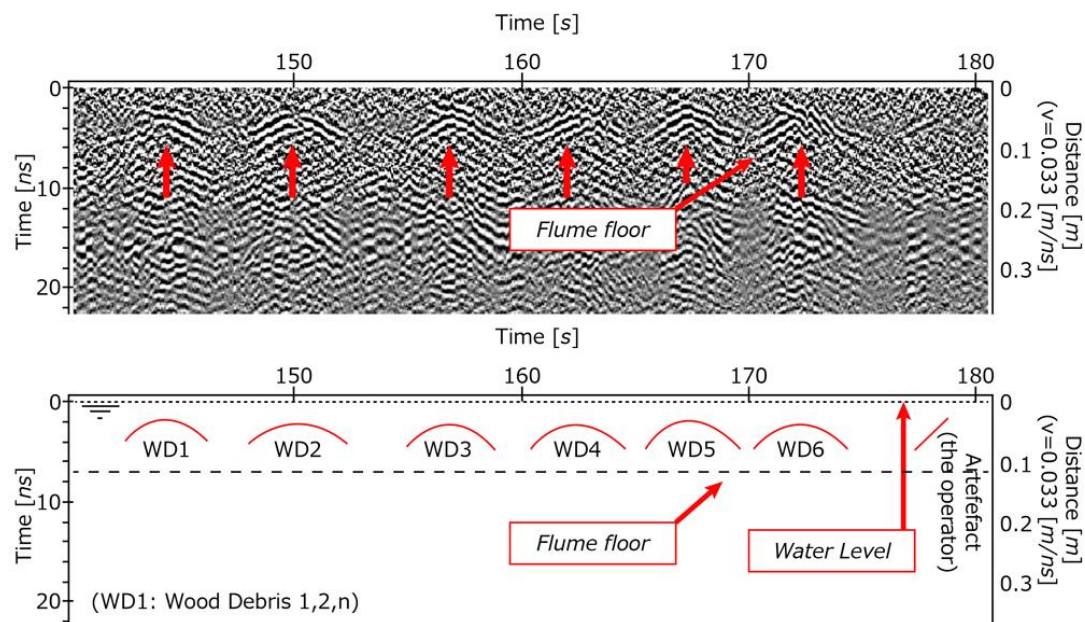


Figure 3. Original radargram after signal processing and explanation of the data extracted.

Table 3. Calculation of velocities based on the hyperbolae slopes of the radargram.

Wood nb	Depth 1 [ns]	Depth 2 [ns]	x1 [1/100s]	x2 [1/100s]	Start sec	time-lapse sec	Triangulated Horizontal [ns]	Halfed (re-turn to single) ns	Nanosec. to distance using light-speed [m]	Velocity [m/s]
1.000	5.045	3.550	14283	14421	0.000	1.380	3.585	1.792	0.520	0.377
1.000	4.718	3.177	14270	14403	0.000	1.330	3.489	1.744	0.506	0.380
2.000	4.205	2.663	14839	14977	0.000	1.380	3.254	1.627	0.472	0.342
2.000	4.251	2.616	14837	14975	0.000	1.380	3.351	1.675	0.486	0.352
3.000	4.999	2.990	15531	15699	0.000	1.680	4.006	2.003	0.581	0.346
3.000	4.111	2.336	16051	16211	0.000	1.600	3.383	1.692	0.491	0.307

* Depth 1 and 2 are the two vertical points from the hyperbolae used for calculation of the velocity; x1 and x2 are the horizontal elements of the same points. Timelapse, is the time between x1 and x2.

4. Conclusion

The experiments shows that (1) wood can be counted from the electromagnetic imaging; (2) the velocity of the wood can also be estimated, although the present experiments need to be run with a longer flume, so that the optimal velocity is attained; (3) finally the

next step in the present research is to compare the falling and rising limb to calculate the acceleration of the wood .

Supplementary Materials: There is no supplementary material

Author Contributions: Conceptualization, methodology and analysis C.G. ; formal analysis, C.G.; N.H.; S.M.; M.K.; K.A.; writing—original draft preparation, C.G.; writing—review and editing C.G.; N.H.; S.M.; F.P.; Grant acquisition: N.H. All authors have read and agreed to the published version of the manuscript.

Funding: This research was supported by the Japanese Grant-in-Aid for Scientific Research Kakenhi-B (22H02383) lead by N.H.

Data Availability Statement: Data available upon request to the corresponding author, and should be made available once further experiments have been conducted

Acknowledgments: The GPR used in the present experiment was acquired from the Japanese Research fund Kakenhi-Kiban-A (18H03957).

Conflicts of Interest: The authors declare no conflict of interest.

References

1. Gunnell, A.M.; Petts, G.E.; Gregory, K.J. The role of coarse woody debris in forest aquatic habitats: implications for management. *Aquat Conserv* **1995**, *5*, 1-24.
2. Bisson, P.A.; Bilby, R.E.; Bryant, M.D.; Dollof, C.A.; Grette, G.B.; House, M.L.; Murphy, M.L.; Koski, K.V.; Sedell, J.R. Large woody debris in forested streams in the Pacific Northwest: past, present and future. In *Streamside Management: Forestry and Fishery Interactions*, Saleo, E.O.; Cuntz, T.W., Eds.; University of Washington Publisher, Washington, USA, 1987.
3. Abbe, T.M.; Montgomery, D.R. Patterns and processes of wood debris accumulation in the Queets river basin, Washington. *Geomorphology* **2003**, *51*, 81-107.
4. Nakamura, F.; Swanson, F.J. Effects of coarse woody debris on morphology and sediment storage of a mountain stream system in western Oregon. *Earth Surf Process Landf* **1993**, *18*, 46-61.
5. Seo, J.; Nakamura, F.; Chun, K. Dynamics of large wood at the watershed scale: a perspective on current research limits and future directions. *Landsc Ecol Eng* **2010**, *6*, 271-287.
6. Chen, S.-C.; Chao, Y.-C.; Chan, H.-C. Typhoon-dominated influence on Wood Debris Distribution and Transportation in a High Gradient Headwater Catchment. *J Mt Sci* **2013**, *10*, 509-521.
7. Moulin, B.; Piegay, H. Characteristics and temporal variability of large woody debris trapped in a reservoir on the river Rhone (Rhône): Implications for river basin management. *Riv Res Appl* **2004**, *20*, 79-97.
8. Thevenet, A.; Citterio, A.; Piegay, H. A new methodology for the assessment of large woody debris accumulations on highly modified rivers (example of two French piedmont rivers). *Regul Rivers: Res Mgmt* **1998**, *14*, 467-483.
9. Shimizu, M.; Kanai, S.; Hotta, N.; Lissak, C.; Gomez, C. Spatial Distribution of Drifted-wood Hazard following the July 2017 Sediment-hazards in the Akatani river, Fukuoka Prefecture, Japan. *For Geo* **2020**, *34*, 96-111.
10. Pettit, N.E.; Warfe, D.M.; Kennard, M.J.; Pusey, B.J.; Davies, P.M.; Douglas, M.M. Dynamics of in-stream wood and its importance as fish habitat in a large tropical floodplain river. **2013**, *29*, 864-875.
11. Bocchiola, D.; Rulli, M.C.; Rosso, R. Flume experiments on wood entrainment in rivers. *Adv Water Resour* **2006**, *29*, 1182-1195.
12. Panici, D. An Experimental and Numerical Approach to Modeling Large Wood Displacement in Rivers. *Water Resour Res* **2012**, *57*, 1-18.
13. Spreitzer, G.; Gibson, J.; Tang, M.; Tunnicliffe, J.; Friedrich, H. SmartWood: Laboratory experiments for assessing the effectiveness of smart sensors for monitoring large wood movement behaviour. *Catena* **2019**, *182*, 104145, 1-15.
14. Ravazzolo, D.; Mao, L.; Pico, L.; Lenzi, M.A. Tracking log displacement during floods in the Tagliamento River using RFID and GPS tracker devices. *Geomorph* **2015**, *228*, 226-233.
15. Ghaffarian, H.; Piegay, H.; Lopez, D.; Riviere, N.; MacVicar, B.; Antonio, A.; Mignot, E. Video-monitoring of wood discharge: first inter-basin comparison and recommendations to install video cameras. *Earth Surf Process Landforms* **2020**, *45*, 2219-2234.
16. MacVicar, B.; Piegay, H. Implementation and validation of video monitoring for wood budgeting in a wandering piedmont river, the Ain River (France). *Earth Surf Process Landforms* **2012**, *37*, 1272-1289.
17. Galley, R.J.; Trachtenberg, M.; Langlois, A.; Barber, D.G.; Shafai, L. Observations of geophysical and dielectric properties and ground penetrating radar signatures for discrimination of snow, sea ice and freshwater ice thickness. *Cold Reg Sci Technol* **2009**, *57*, 29-38.
18. Jaedicke, C. Snow mass quantification and avalanche victim search by ground penetrating radar. *Surv Geophys* **2003**, *24*, 431-445.
19. Huber, E.; Birte, A.; Huggenberger, P. Imaging scours in straightened and braided gravel-bed rivers with ground-penetrating radar. *Near Surf Geophys* **2019**, *17*, 263-276.

20. Bakker, M.A.J.; Maljers, D.; Weerts, H.J.T. Ground-penetrating radar profiling on embanked floodplains. *Neth J Geosci* **2007**, *86*, 55-61.
21. Wyatt, D.E.; Temples, T.J. Ground-penetrating radar detection of small-scale channels, joints and faults in the unconsolidated sediments of the Atlantic Coastal Plain. *Env Geol* **1999**, *27*, 219-225.
22. Lissak, C.; Maquaire, O.; Malet, J.-P.; Lavigne, F.; Virmoux, C.; Gomez, C.; Davidson, R. Ground-penetrating radar observations for estimating the vertical displacement of rotational landslides. *Nat Hazards Earth Syst Sci* **2015**, *15*, 1399-1406.
23. Kain, C.; Gomez, C.; Wassmer, P.; Lavigne, F.; Hart, D. Truncated dunes as evidence of the 2004 tsunami in North Sumatra and environmental recovery post-tsunami. *N Z Geogr* **2014**, *70*, 165-178.
24. Starheim, C.A.; Gomez, C.; Harrison, J.; Kain, C.; Brewer, N.J.; Owen, K.; Hadmoko, D.S.; Purdie, H.; Zavar-Reza, P.; Owens, I.; Wassmer, P.; Lavigne, F. Complex internal architecture of a debris-flow deposit revealed using ground-penetrating radar, Cass, New Zealand. *N Z Geogr* **2013**, *69*, 26-38.
25. Gomez, C.; Lavigne, F.; Lespinasse, N.; Hadmoko, D.S.; Wassmer, P. Longitudinal structure of pyroclastic-flow deposits, revealed by GPR survey, at Merapi Volcano, Java, Indonesia. *J Volcanol Geotherm Res* **2008**, *176*, 439-447.
26. Guo, S.; Xu, Z.; Li, X.; Zhu, P. Detection and Characterization of Cracks in Highway Pavement with the Amplitude Variation of GPR Diffracted Waves: Insights from Forward Modeling and Field Data. *Remote Sens* **2022**, *14*, 1-16.
27. Hugenschmidt, J. Concrete bridge inspection with a mobile GPR system. *Constr Build Mat* **2002**, *16*, 147-154.
28. Granlund, N.; Lundberg, A.; Feiccabrino, J.; Gustafsson, D. Laboratory test of snow wetness influence on electrical conductivity measured with ground penetrating radar. *Hydrol Res* **2009**, *40*, 33-44.